# Impact of lower plate structure on upper plate deformation at the NW Sumatran convergent margin from seafloor morphology

David Graindorge, Frauke Klingelhoefer, Jean-Claude Sibuet, Lisa Mcneill, Timothy J. Henstock, Simon Deanc, Marc-André Gutscher, Jean Xavier Dessa, Haryadi Permana, Satish C. Singh, et al.

# Impact of lower plate structure on upper plate deformation at the NW Sumatran convergent margin from seafloor morphology

David Graindorge[a, *], Frauke Klingelhoefer[b], Jean-Claude Sibuet[b], Lisa McNeill[c], Timothy J. Henstock[c], Simon Dean[c], Marc-André Gutscher[a], Jean Xaver Dessa[d], Haryadi Permana[e], Satish C. Singh[f], Hélène Leau[g], Nicolas White[h], Hélène Carton[f], Jacques André Malod[a], Claude Rangin[i], Ketut G. Aryawan[j], Anil Kumar Chaubey[k], Ajay Chauhan[f], Dodi R. Galih[e], Christopher James Greenroyd[l], Agus Laesanpura[m], Joko Prihantono[n], Gillian Royle[f] and Uma Shankar[o]

[a] UMR 6538 Domaines Océaniques UBO/IUEM, Technopôle Brest-Iroise, Place Nicolas Copernic, F-29280 Plouzané, France
[b] Ifremer, Brest, France
[c] National Oceanography Centre, University of Southampton, Southampton, UK
[d] UPMC, UMR Géosciences-Azur, Nice, France
[e] Earth Dynamics and Geological Disaster Division, Research Center for Geotechnology, Indonesia Institute of Sciences, Bandung, Indonesia
[f] Institut de Physique de Globe de Paris (IPGP), Paris, France
[g] Institut Polaire Paul Emile Victor (IPEV), Brest, France
[h] Bullard Laboratories, Cambridge, UK
[i] Collège de France/CNRS, Aix en Provence, France
[j] Marine Geological Institute, Energy and Earth Resources Department, Bandung, Indonesia
[k] National Institute of Oceanography, Goa, India
[l] Durham University, Durham, UK
[m] ITB, Bandung, Indonesia
[n] Marine and Fishery Department, Pasir Putih, Jakarta, Indonesia
[o] NGRI, Hyderabad, India

*: Corresponding author : Graindorge D., email address : David.Graindorge@univ-brest.fr

---

**Abstract:**

We present results from multibeam bathymetric data acquired during 2005 and 2006, in the region of maximum slip of the 26 Dec. 2004 earthquake (Mw 9.2). These data provide high-resolution images of seafloor morphology of the entire NW Sumatra forearc from the Sunda trench to the submarine volcanic arc just north of Sumatra. A slope gradient analysis of the combined dataset accurately highlights those portions of the seafloor shaped by active tectonic, depositional and/or erosional processes. The greatest slope gradients are located in the frontal 30 km of the forearc, at the toe of the accretionary wedge. This suggests that long-term deformation rates are highest here and that probably only minor amounts of slip are accommodated by other thrust faults further landward. Obvious N–S oriented lineaments observed on the incoming oceanic plate are aligned sub-parallel to the fracture zones associated with the Wharton fossil spreading center. Active strike-slip motion is suggested by recent deformation with up to 20–30 m of vertical offset. The intersection of these N–S elongated bathymetric scarps with the accretionary wedge partly controls the geometry of thrust anticlines and the location of erosional features (e.g. slide scars, canyons) at the wedge toe. Our interpretation suggests that these N–S lineaments have a significant impact on the oceanic plate, the toe of the wedge and further landward in the wedge. Finally, the bathymetric data indicate that folding at the front of the accretionary wedge occurs primarily along landward-vergent (seaward-dipping) thrusts, an unusual style in accretionary wedges worldwide. The N–S elongated lineaments locally act as boundaries between zones with predominant seaward versus landward vergence.

**Keywords:** subduction; accretionary wedge; seafloor morphology; tectonic; Sumatra

## 1. Introduction

The 26 December 2004 East Indian Ocean earthquake (Mw 9.2) was the biggest earthquake recorded in the past 40 years and generated the largest far-field (trans-oceanic) tsunami ever monitored (Merrifield et al., 2005). This subduction megathrust earthquake triggered an average ~ 10 m slip along a 1300 km long segment of the plate boundary between the Indo-Australian plate and the Eurasian (Sunda–Burma) plate (Lay et al., 2005). Rupture initiated at 30–40 km depth, about 50 km north of Simeulue Island, along a segment of the subduction zone which had not experienced a great thrust earthquake M > 8 in the past at least 200 years (Lay et al., 2005) (Fig. 1). Vertical motion of the seafloor and subsequently the water column above generated a tsunami that killed over 250,000 people in Southeast Asia. The earthquake was caused by sudden slip (up to ~ 30 m) releasing the elastic stress accumulated along the subduction zone interface between the Indo-Australian plate and the Sunda–Burma plate (Bilham, 2005), subducting obliquely at a rate of 4–6 cm/yr in a N8–20° azimuth (Vigny et al., 2005 C. Vigny, W.F.J. Simons, S. Abu, R. Bamphenyu, C. Satirapod, N. Choosakul, C. Subarya, A. Socquet, K. Omar, H.Z. Abidin and B.A.C. Ambrosius, Insight into the 2004 Sumatra–Andaman earthquake from GPS measurements on southeast Asia, Nature 436 (2005), pp. 201–206. View Record in Scopus | Cited By in Scopus (86)Vigny et al., 2005).

In the 2 years following this event, a concerted international effort to study the rupture zone of this great earthquake led to several oceanographic expeditions (e.g., [Singh, 2005], [Ladage et al., 2006] and [Henstock et al., 2006]). One of the priorities was to determine the detailed morphology of the seafloor and to delineate the underlying structure in the zone of maximum coseismic slip. A key objective was to map the major tectonic features and in particular to search for evidence of submarine scarps, outcropping faults, slide scars etc., geologically reflecting

(geologically) recent deformation of the margin interacting with longer term processes. We present here analysis of combined bathymetric dataset acquired by HMS Scott (January-February 2005), and R/V Marion Dufresne (July-August 2005, and July-August 2006). These data provide high resolution images of the seafloor morphology offshore Sumatra, covering the deep oceanic domain, the accretionary wedge, forearc basin, Sumatran shelf and offshore extension of the strike-slip Sumatran Fault.

**2. Datasets and Processing**

The R/V Marion Dufresne is equipped with a deep water multibeam echosounder (MBES) Seafalcon 11 developed by Thales Underwater System. The echo-sounder uses 400-500 beams on 5 planes at 12 kHz frequency along a 120° fan. The lateral resolution varies with depth and is typically equal to depth/100. The survey was carried out at a mean speed of 14 knots. Positions were computed in the geodetic system WGS 84. Sound velocities were obtained using regularly spaced SIPPICAN Temperature Expendable probes (XBT's) processed manually with CARAIBES software on board. The HMS Scott is equipped with a high-precision deep water multibeam echosounder, jointly developed by the United States Navy and SeaBeam Instruments Inc : the SASS IV system (Sonar Array Sounding System) with 361 beams and a 120° swath width. It is a 12 kHz frequency high resolution multibeam sonar system, with vertical resolution of ~5 m and deep-water horizontal resolution up to ~25 m (Henstock et al., 2006). To obtain uniform data coverage, the combined were mapped to a 90 m spacing grid.

Sub-bottom profiler (very high resolution seismic) data were acquired using the Marion Dufresne's Thomson Marconi TSM 5265 MBES combined multibeam echosounder and sub-bottom profiler (SBP), with Thales Sea Falcon 11 software. The SBP data was acquired using 3.75 kHz frequency chirp source wavelet. Data were recorded in SEG-Y format at 0.417 ms sample rate and 400 ms fixed trace length (960 samples per trace). The original shot interval is 20 sec, then spacing between traces varies from 30 to 100 m depending on the vessel speed which varied from 14 knots during the bathymetric survey to 4.5 knots during the seismic survey. Thus data from the SBP were binned/interpolated to a 75 m for regular spacing.

**3. General Morphology of NW Sumatra fore-arc**

The bathymetric compilation resulting from the three cruises, provides a high resolution image of the seafloor at a 90 m grid spacing over a region of roughly 3.5° x 2.5°, an area of approximately 100,000 $km^2$. The map extends from the trench off Simeulue and the entire forearc off northwestern Sumatra to the Andaman Sea north of Sumatra and to the Indonesian-Indian boundary to the north-west (Figure 1). Coverage is over 80% in the central region (93-95°E, 2.5-5°N) that laterally includes the epicenter (position of rupture initiation) of the 26 December 2004 earthquake. The region can be divided into five tectonic provinces across the margin from SW to NE:

1) The flat, relatively undeformed oceanic plate and trench. This domain consists of a flat nearly featureless abyssal plain at depths of 4300-4900 m, with an extremely gentle slope towards the east, terminating at the foot of the accretionary wedge. A distinct morphologic "trench" is barely observable because it is filled with sediments. Thickness of sediments at the "trench" reaches 2-3 sec. two way travel time along the northern Sumatra trench (Moore and Curray, 1980, Segoufin et al., 2004, Singh et al., 2006; Gaedick et al., 2006). A few, subtle, lineaments and a series of en echelon depressions are observed, aligned in a N-S to N15E direction, consistent with the orientation of fracture zones related to the Wharton fossil spreading center (Deplus et al., 1998).

2) The accretionary wedge. The lowermost forearc consists of a series of elongate ridges, aligned sub-parallel to the trench, with an average spacing of 5-15 km, and a typical vertical relief of 200-1000 m (e.g., Henstock et al., 2006). Within 20-40 km of the trench, the seafloor rises over 3000 m to attain depths of about 1500 m. The next 100 km towards the NE consists of a plateau, with mean water depths of 1000-2000 m, marked by about 8-10 elongate ridges and intervening troughs parallel to the subduction front. This high rugosity region has a NE termination along a feature termed "outer arc ridge" by Karig et al. (1980) which forms the boundary of the Aceh forearc basin. Within the north-eastern flank of the ridge we also observe the linear right-lateral West Andaman Fault (Izart et al., 1994; Malod et al, 1996; Curray, 2005; Singh et al., 2005) which might be northward extension of the Mentawai fault off central-south Sumatra (Diament et al, 1992). Further south this system becomes more complex. The relarively shallow water (less than 1000 m) Simeulue plateau (North West of Simeulue) is possibly linked to the outer-arc high forming the western flank of the Aceh basin. Then, the accretionary wedge shows a global narrowing from the NW (120 km of the Aceh Basin) to the SE (60 km of Simeulue Island).
3) The Aceh forearc basin lies landward of the accretionary wedge plateau and is marked by a generally smooth, flat seafloor at a mean depth of 2500 m. The Simeulue Basin further southeast is a shallower basin with a mean depth of about 1000 m, and is divided into two sub-basins by a structural high at ~800 m (Neben et al., 2006) previously associated with the Mentawai fault (Izart et al., 1994). The forearc basins typically have a width of 20-50 km. The Aceh and Simelue basins are separated by a WNW-ESE trending structural high previously interpreted as the Tuba ridge (Malod et al., 1993; Curray, 2005).
4) The upper continental slope and shelf of Sumatra, has a width of 20-50 km. It is widest (40-50 km) off the NW tip of Sumatra, with a generally smooth but west dipping slope of a few degrees. It is locally incised by canyons transporting terrestrial sediments into the forearc basin.
5) The Sumatra-Andaman submarine arc trough north of Sumatra is composed of several predominantly right-lateral strike-slip faults as part of the northern prolongation of the Sumatran and Seulimeu faults (Malod et al., 1993; Mustafa Kemal, 1993; Sieh and Natawidjaja, 2000). To the west of the volcanic axis, there are two major faults with down to the NE movement (normal or transtensional) and one major fault to the east. These bound a deep trough (water depths of 3000-3600 m) with submarine volcanic edifices located in the central axis of this deep basin.
In this article we will focus mainly on the 2 first domains.

**4. Sea-floor slope and morpho-tectonic maps**

We have calculated the sea floor slope from the combined bathymetry dataset (Figure 2). The maximum slope provides clues as to which portions of the seafloor are being shaped by active processes (tectonic, sedimentary, gravitational). It also provides an estimate of the mechanical properties of the seafloor strata (e.g. coefficient of internal friction, which affects slope stability). The steepest slopes in the region (>15-20°) are found along the flanks of the elongate accretionary wedge thrust ridges (particularly at the toe of wedge where we suggest active deformation is focused), along canyons incised into the upper and lower portions of the margin and locally along the edges of landslide scars. All slopes greater than 20° can be considered to be potentially unstable.

A morphotectonic map was constructed (Figure 3) using seafloor morphology, the calculated slopes, and the 3.5kHz seismic data. Features with slopes >5° indicate potentially active structures, e.g., as blind thrusts, surface-breaking faults or submarine canyons. The interpretation of the widespread elongate sub-parallel ridges and related landward and seaward vergent thrusts (Henstock et al., 2006) is based on the geodynamic setting of the

accretionary wedge where thrust (fault bend fold) type anticlines are commonly observed in nature (Suppe, 1983; Flueh et al., 1998), analogic models (Gutscher et al., 1998) and seismic data from the region (e.g., Singh et al., 2006; Sibuet et al., 2007; Franke et al., 2006 and Gaedicke et al., 2006). On Figure 3, we mark thrusts and discontinuities in the fold axes with different symbols based on there clarity.

**5. The oceanic plate and N-S Lineaments**

On the flat-lying oceanic plate outboard of the trench, the bathymetry data reveal a set of N-S to N 15°E trending lineaments (figure 3) which are also clearly observed on the high-resolution seismic profiles (SBP) acquired during the RV Marion Dufresne Sumatra-OBS cruise (Figures 4 and 5). One of the most prominent N-S lineaments, near 92.8°E, is over 50 km long and has vertical offset of 10-30 m towards the east on several 3.5 kHz profiles (Figure 4). Smaller graben-type features (typically 10 m in height) can be observed parallel to this major N-S scarp. This overall geometry and the general deepening of the seafloor to the east are consistent with a pattern of normal faulting or at least dip-slip component of strike-slips faults (Figure 4).

Further south near 94.1°E, a pair of sub-parallel lineaments are observed, with orientations of N4°E and N10°E, respectively (Figure 5). The western of the two consists of a series of en echelon elongate N-S basins reminiscent of pull-apart basins formed by transtensional motion along an interpreted system of left-lateral strike slip faults (Figure 5a). The surface expressions in the 3.5 kHz profiles are variable, ranging from 20-40 m steps, and locally, small 10 m deep clefts.

Previously recognized major features on the oceanic plate between the Ninety east and the Investigator ridges (Hebert et al., 1996) to the South-east of Sumatra are fracture zones in the Wharton Basin activated and reactivated as left-lateral N-S strike-slip faults (Deplus et al., 1998) due to deformation in the India-Capricorn-Australia plate system (Gordon et al., 1998). Their orientation is typically N 5°E, sub-parallel to the lineaments observed near the Sumatra trench at 92.8°E and 94.1°E (Figures 4 and 5). Similarly, prominent fracture zones are visible in free-air gravity (Figure 6) and magnetic data although the potential field data do not have sufficient resolution to constrain precisely the locations of their intersection with the trench.

Active minor faults and lineations are frequently observed deforming the subducting oceanic plate in the vicinity of subduction zone trenches for example in Central America (Ranero et al, 2003 a and b) and South America (Weinrebe et al., 2003 ; von Huene and Ranero, 2003). Such lineaments most commonly represent normal faults, induced by flexure of the oceanic plate outboard of the trench, such as those observed in Central America (Ranero et al, 2003 a and b) and South America (Weinrebe et al., 2003 ; von Huene and Ranero, 2003). The faulting pattern caused by bending of the oceanic plate can exhibit a wide variation of orientations (Ranero et al., 2005), but they are typically sub-parallel or slightly oblique to the trench orientation. In Central Chile, two populations of faults are seen, one sub-parallel and another strongly oblique to the trench (Ranero et al., 2005). The faulting pattern offshore Chile is particularly well expressed, in large part due to the very thin cover of sediments (100 m) overlying the igneous oceanic crust. The fault pattern is controlled in part by the pre-existing crustal fabric and planes of weakness within the incoming plate, as it is subjected to trench perpendicular bending stresses (Ranero et al., 2005).

Off NW Sumatra the primary fabric of the oceanic crust (normal faults parallel to the ancient spreading center) is at a high angle (50-60°) to the trench axis (Figure 6), and is unfavorably oriented for possible reactivation. The large-scale features observed in the Wharton Basin are the Ninety East Ridge and Investigator Ridges and a set of sub-parallel fracture zones that are often associated with strike-slip focal mechanisms, producing a pervasive N-S fabric (Figure 6; Deplus et al., 1998). The N5°E lineations observed west of

North Sumatra appear to be expressions of this oceanic plate fabric (fracture zone related). In the northern sub-region (~92.8°E) these lineaments are oriented at an angle of 25° with respect to the deformation front (Figure 4). These features are continuation of the strike slip faults observed by Deplus et al., 1998 (Figure 6), but the structural style observed suggests these lineations are reactivated as normal faults due to flexural bending of the oceanic plate in the vicinity of the trench, although the spacing between the lineations is much less than the typical spacing of fracture zones within the region. Other studies have indicated that when pre-existing faults are oriented at an angle of less than 30° to the trench axis, these faults will be reactivated, and that no new sets of normal faults will develop (Ranero et al., 2005, Masson, 1991). The N-S trending scarps and graben we observe are consistent with this process of formation. Fault plane solutions offshore NW Sumatra show only few evidences of normal faulting in the oceanic plate (Figure 6 : normal events have been suppressed on the "continental" frontal arc domain) during the last 30 years. Most of the earthquakes reported postdate the December 2004 event. Normal fault plane solutions are similarly scarce on the oceanic domain in middle America and Central Chile (Ranero et al., 2005).

In the southern sub-region (94.1°E), the N5°E trending fabric is at a very high angle to the trench (>60°) due to the curvature of the deformation front (Figure 1). Mechanically, any weaknesses with this orientation are unlikely to be reactivated as normal faults. However, there is a family of NNW-trending (N150°-160°E) troughs and scarps (black dotted lines in Figure 3 and Figure 5) we interpret to be structurally-derived and which are oriented at an angle of about 35° to the local deformation front. Given the overall curvature of the Sumatra margin here, their orientation may be an expression of the far-field plate bending stresses, which could be generating a new set of normal faults. The N4°E trending lineament, with the en-echelon basins shows evidence of activation as a system of strike-slip faults (Figure 5a). Given the shape and offset of the basins, the sinistral fault-motion is favorised (Figure 5a). Fault plane solutions from the oceanic domain offshore NW Sumatra confirm sinistral strike-slip faulting in the oceanic plate (Figure 6). Active sinistral strike-slip deformation was also observed near the Wharton Fossil spreading center (Deplus et al., 1997).

For both the northern and southern sub-regions off NW Sumatra, it is important to note that the igneous oceanic crust is overlain by up to ~3 km or more thickness (Segoufin et al., 2004) or alternatively up to 3.5 sec TWT (Gaedicke et al., 2006) of hemi-pelagic sediment and trench fill. Thus, the fact that the seafloor is offset by faults with a vertical throw of 30m indicates significant, active deformation related to basement faulting.

**6. The accretionary wedge**

The lower part of the accretionary wedge is characterized by a rapid change in depth from the adjacent oceanic basin and deformation front (mean depth ~4600m) to an undulating plateau with mean water depths oscillating from 1000 to 2000 m. At the most seaward 20-40 km of the wedge, where the steepest slopes are found (locally over 20°), the seafloor rises by 3000 m over a series of 2-3 trench sub-parallel elongated ridges (folds) with an average spacing of 5-15 km. This style of deformation is present along ~70% of the wedge toe surveyed in this study (morphology A of Henstock et al., 2006) and the remaining 30% (red arrow on figure 3) is characterized by a lack of such folds (morphology B of Henstock et al., 2006; McNeill et al., 2006).

In the part of the front characterized by elongated thrust folds (A), the slope gradient map (Figure 2) highlights the asymmetry of the 1-2 frontal folds which are segmented along the trench into 25-100 km long structures The steepest slopes are commonly observed on the landward side of the thrust anticline, with the more gentle (bedding parallel) slope on the seaward side. Similarly, 3.5kHz data documents the asymmetry of the frontal fold attaining a vertical relief of 200-1000 m from the surrounding seafloor. This is caused by the seaward

tilting of strata during slip along the primary (seaward-dipping or landward vergent) fault (Henstock et al., 2006). Landward-vergent thrusting is a rare phenomenon, which is best documented for the Cascadia margin (MacKay et al., 1992 ; Gutscher et al., 2001). The variation of structural style (i.e. seaward versus landward) in Cascadia reflects a regional change in both sediment type and rate of deposition that affect the potential for overpressure in the sediments (MacKay, 1995). The presence of landward vergence here is particularly associated with the development of submarine fans (i.e. Astoria and Nitinat) (Fisher et al., 1999). Along the northern Sumatra margin the presence of landward vergence in part coincides with an area of a possible paleo Bengal fan prior to the subduction of the Ninety East ridge (Figure 3; McNeill et al., 2006). However, even where landward vergence dominates, a conjugate seaward-verging fault commonly develops with time (Franke et al., 2006). In the other part of the margin (B) where no elongated thrust folds are present, the major thrusts at the deformation front may be landward–dipping, as proposed on the interpreted map. These interpretations are partially supported by seismic data collected to date (Mosher et al., 2005; Franke et al., 2006).

Higher up in the wedge, based on morphological criteria, we interpret that landward-dipping thrusts become dominant as seems to be supported by recent seismic data (Franke et al., 2006, Singh et al., 2006), which. This finally leads to a pattern of doubly-verging elongated folds separated by troughs or elongated valleys possibly representing piggy-back basins (Sibuet et al., submitted). The 6-8 elongated folds are discontinuous with fold crest elevations of 800-1200 m, spacing up to 5-25 km, and segment lengths of 20-110 km long (Figure 3, see also Henstock et al., 2006) separated by short 10 to 35 km long N-S lineaments, which appear as N-S elongated valleys. The interaction of N-S oriented lineaments with fold axes is expressed by a sigmoid morphologic pattern of ridges and troughs (Figure 3: 4.7°N and 93.65°E) and may be the expression of distributed dextral deformation within the wedge related to oblique convergence. Earthquake focal mechanisms (during and after the 2004 main shock, Figure 6) show little evidence of mainly left lateral strike-slip motion in the study area which represent an interseismic decoupled ongoing deformation of the Indo-Australian plate, even if some aftershock events are reported to align along N-S trends (Sibuet et al. (subm.) and Sibuet et al., 2006).

**7. Lower plate control of upper plate structures :**

In part A of the toe of the wedge, a series of frontal thrust anticlines observed at 94°E, 3°N exhibit clear lateral segment boundaries, some of which coincide with major observed N-S trending lineaments on the oceanic crust that reach the deformation front (Figures 3)). This is best expressed in the seafloor slope map (Figure 2) and in the 3-D perspective view (Figure 7). Other segment boundaries may be partly by controlled by minor structures not reaching the seafloor or other as yet unidentified processes. Furthermore, the intersection of the N-S elongated bathymetric relief with the deformation front of the accretionary wedge appears to locally control the location of many of the local canyon/complex slump systems which incise the slope and frontal few folds.

On the Sumatra deformation front, we observe a more localized impact of the N-S elongated scarps associated with the pervasive N-S fabric of the Indo-Austalian plate (Figure 6) than has been argued for in Cascadia (e.g., MacKay et al., 1992; Goldfinger et al., 1997). In Cascadia, at 45°N the structural changes from seaward vergence in the South to landward vergence in the North appear to be bounded by WNW trending left lateral strike slip faults (MacKay et al., 1992, 1995). Some of these faults cut the Juan de Fuca plate and can be traced into the North American plate; they probably originate from Juan de Fuca plate and propagate into the overlying fore arc (Goldfinger et al., 1992, 1997). However the N-S observed faults may locally juxtapose sediments with different physical properties, and act as fluid conduits,

both phenomena resulting in stepwise changes in pore pressure. As previously recognized on the Cascadian margin (MacKay, 1995), this process may locally (Figure 3: 3°N, 94°E and Figure 7) control the structural style of the Northern Sumatra margin deformation front, for example, propagation of strike slip faults into the upper plate may reduce pore fluid pressure, increase coupling and then trigger evolution from landward to seaward vergence (Johnson et al., 2004, 2007). Higher up in the Sumatran wedge, the sigmoid deformation pattern and the N-S valleys previously described could also be related to the N-S lower plate active strike slip faults.

**8. Conclusion**

High-resolution multibeam bathymetric images from the source region of the 26 December 2004 Sumatra earthquake reveal active processes shaping the seafloor. The region of steepest slopes is in the frontal 30 km of the wedge and indicates that the majority of active long-term compressive deformation is focused here. N-S oriented lineaments are observed on the downgoing oceanic plate, which are related to the fracture zone fabric of the oceanic crust. These structures contribute to controlling segmentation of structures in the upper plate and the locations of slope failure.

**Acknowledgments**

Thanks to the Captain and the crew of the R/V Marion Dufresne and Royal Navy HMS Scott. We gratefully acknowledge financial support from the French ANR Program through the SAGER project and the Indonesian Government for permission to carry out the surveys. Most of the figures were drafted using GMT software (Wessel and Smith, 1991). This paper is IUEM contribution number XXXX.

**References**


Bilham, R., 2005. A Flying Start, Then a Slow Slip, Science, v. 308, p. 1126 - 1127.

Curray, J.R., 2005. Tectonics and history of the Andaman Sea region, Journal of Asian Earth Sciences, v. 25, Issue 1, p. 187-232.

Deplus, C., Diament, M., Hebert, H., Bertrand, G., Dominguez, S., Dubois, J., Malod, J., Patriat, P., Pontoise, B., Sibilla, J.-J., 1998. Direct evidence of active deformation in the eastern Indian oceanic plate. Geology, v. 26, p. 131-134.

Diament, M., Harjono, H., Karta, K., Deplus, C., Dahrin, D., Zen, M. T., Gerard, M., Lassal,O., Martin, A., and Malod, J., 1992. Mentawai fault zone off Sumatra; a new key to the geodynamics of western Indonesia, Geology; March 1992, v. 20, no. 3, p. 259-262.

Fisher, M. A., Flueh, E. R., Scholl, D. W., Parsons, T., Wells, R. E., Trehu, A., ten Brink, U., and Weaver, C. S., 1999. Geologic processes of accretion in the Cascadia subduction zone west of Washington State, Geodynamics, v. 27, p. 277-288.

Flueh, E.R., Fisher, M.A., Bialas, J., Childs, J.R., Klaeschen, D., Kukowski, N., Parsons, T., Scholl, D.W., ten Brink, U., Tréhu, A.M., and Vidal, N., 1998. New seismic images of the Cascadia subduction zone from cruise SO108 — ORWELL, Tectonophysics, v. 293, Issues 1-2, p. 69-84.

Franke, D., Gaedicke, C., Ladage, S., Tappin, D., Neben, S., Ehrhardt, A., Mueller, C., and Djajadihardja, Y., 2006. Contrasting styles of deformation along the Sumatra subduction zone, EOS Trans. Amer. Geophys. Union, v. 87, n. 52, AGU Fall Meeting, Abstract U53A-0017.

Gaedicke, C., Franke, D., Ladage, S., Tappin, D., Baranov, B., Barkhausen, U., Berglar, K., Delisle, G., Djajadihardja, Y., Heyde, I., Lutz, R., Khafid, K., Mueller, C., Nur Adi, K., Park, J., Seeber, L., Neben, S., and Triarso, E., 2006. Imaging the rupture areas of the giant northern Sumatra earthquakes : a multidisciplinary geophysical experiment, EOS Trans. Amer. Geophys. Union, v. 87, n. 52, AGU Fall Meeting, Abstract U52A-01.

Goldfinger, C., Kulm, L.D., Yeats, R.S., Appelgate, B., MacKay, M., and Moore, G.F. 1992. Transverse structural trends along the Oregon convergent margin: implications for Cascadia earthquake potential, Geology, v. 20, p. 141-144.

Goldfinger, C.,Kulm, L. D., Yeats, R. S., Hummon, C., Huftile, G. J., Niem, A. R., and McNeill, L. C., 1996. Oblique strike-slip faulting of the Cascadia submarine forearc : The Daisy Bank fault zone off central Oregon *in* Subduction top to bottom, Amer. Geophys. Union Geophys. Monogr, v. 96, p. 65-74.

Goldfinger, C., Kulm, L.D., Yeats, R.S., McNeill, L., and Hummon, C., 1997. Oblique strike-slip faulting of the central Cascadia submarine forearc. Journal of Geophysical Research, v. 102, no. B4, p. 8217-8243.

Gordon, R. G., DeMets, C. & Royer, J.-Y., 1998. Evidence for long-term diffuse deformation in the equatorial Indian Ocean, Nature, 395, 370-374.

Gutscher, M.-A., Kukowski, N., Malavieille, J., and Lallemand, S., 1998. Episodic imbricate thrusting and underthursting : Analog experiments and mechanical analysis applied to the Alaskan accretionary wedge. Journal of Geophysical Research, v. 103, p. 10161-10176.

Gutscher, M.-A., Klaeschen, D., Flueh, E.R. and Malavieille, J., 2001. Non-Coulomb wedges, wrong-way thrusting, and natural hazards in Cascadia, Geology, v. 29, p. 379-382.

Henstock, T.J., McNeill, L.C., and Tappin, D., 2006. Seafloor morphology of the Sumatran subduction zone : Surface rupture during a mega-thrust earthquakes?, Geology, v. 34, p. 485-488.

Hébert, H., Deplus, C., and Diament, M., 1996. Origin of the $90^{E}$ Ridge and the investigator Ridge deduced from the analysis of bathymetric and gravity data. C r. Acad. sci., Sér. 2, Sci. terre planet., v. 323, No. 2, p. 105-112.

IOC, IHO and BODC, 2003. "Centenary edition of the GEBCO Digital Atlas", published on CD-ROM on behalf of the Intergovernmental Oceanographic Commission and the International Hydrographic Organization as part of the General Bathymetric Chart of the Oceans; British Oceanographic Data Centre, Liverpool.

Izart, A., Mustafa Kemal, B., and Malod, J.A., 1994, Seismic stratigraphy and subsidence evolution of the northwest Sumatra fore-arc basin. Marine Geology, v. 122, p. 109-124.

Johnson, J.E., Goldfinger, C., Bangs, N.L., and Tréhu, A.M., in revision 2007. Structural vergence variation and clockwise block rotation in the Hydrate Ridge region, Cascadia accretionary wedge offshore Oregon, Tectonics.

Johnson, J.E., Goldfinger, C., Bangs, N. L., Tréhu, A.M., Chevallier, J., 2004. Structural vergence variation and clockwise block rotation in the Cascadia accretionary wedge, offshore central Oregon. Eos Trans. AGU, 85(47), Fall Meet. Suppl., Abstract T41C-1235.

Karig, D.E., M.B. Lawrence, G.F. Moore, and J.R. Curray, 1980. Structural framework of the fore-arc basin, NW Sumatra. J. Geol. Soc. London, v. 137, p. 77-91.

Ladage, S., Gaedicke, C., Djajadihardja, Y., 2006. Great Sumatran earthquakes: MCS images and bathymetry offshore Sumatra - first results of SEACAUSE2 Leg1 cruise SO186, Proc. EGU Meeting, Vienna April 2006. Geophys. Res. Abstr., v.8, 06774.

Lay, T., H. Kanamori, Ammon, C.J., Nettles, M., Ward, S.N., Aster, R.C., Beck, S.L., Bilek, S.L., Brudzinski, M.R., Butler, R., DeShon, H.R., Ekstrom, G., Satake, J., and Sipkin, S., 2005. The Great Sumatra-Andaman earthquake of 26 December 2004, Science, v. 308, p. 1127-1133.

MacKay, M. E., Moore, G. F., Cochrane, G. R., Moore, J. C., Kulm, L. D., 1992. Landward vergence, oblique structural trends, and tectonic segmentation in the Oregon margin accretionary prism, Earth Planet. Sci. Lett., v. 109, p. 477-491.
MacKay M. 1995. Structural variation and landward vergence at the toe of the Oregon accretionary prism, Tectonics, v. 14, No. 5, p. 1309-1320.

Malod, J.-A., B. and B. Mustafa Kemal, 1996. The Sumatra margin : oblique subduction and lateral displacement of the accretionary prism, from Hall, R. & Bluendell, D. (eds), in Tectonic evolution of Southeast Asia, Geol. Soc. Special Publication, No. 106, p. 19-28.

Malod, J.-A., B. Mustafa Kemal, M.-O. Beslier, C. Deplus, M. Diament, K. Karta, A. Mauffret, P. Patriat, M. Pubellier, H. Regnault, P. Aritonang, and M.T. Zen Jr., 1993. Déformations du basin d'avant-arc au Nord-Ouest de Sumatra : une réponse à la subduction oblique. C. R. Acad. Sci. Paris, t. 316, Série II, p. 791-797.

Masson, D.G., 1991. Fault patterns at outer trench walls, Marine Geophysical Research, v. 13, p. 209-225.

McNeill, L., Henstock, T., Tappin, D., Curray, J., 2006. Forearc morphology and thrust vergence, Sunda subduction zone. EOS Trans. Amer. Geophys. Union, v. 87, n. 52, AGU Fall Meeting, Abstract U44A-07.

Merrifield, et al., 2005. Tide gauge observations of the Indian Ocean tsunami, 26 December, 2004. Geophysical Research Letters, v. 32, doi:10.1029/2005GL022610.

Moore, G. F. and R. C. Curray, 1980. Structure of the Sunda trench lower slope off Sumatra from multichannel seismic reflection data. Marine Geophysical Research, v. 4, p. 319-340.

Mosher, D. C., Austin, J. A., Saustrup, S., Fisher, D. and Moran, K., 2005. High-resolution seismic reflection images crossing the Sumatran seismogenic zone: Sumatra Earthquake And Tsunami Offshore Survey (SEATOS), 2005. EOS Trans. Amer. Geophys. Union, v. 86, n. 52, AGU Fall Meeting, Abstract U14A-05.

Mustafa Kemal, B., 1993. La marge active au Nord Ouest de Sumatra. Mécanismes géodynamiques de transfert liés à la subduction oblique, Thèse de Doctorat de l'Université Pierre et Marie Curies, No. 93.17, 165 p.

Neben, S.,Franke, D., Gaedicke, C., Ladage, S., Berglar, K., Damm, V., Ehrhardt, A., Heyde, I., Schnabel, M., and Schreckenberger, B., 2006. Project SUMATRA: The Fore-arc Basin System of Sumatra. Amer. EOS Trans. Amer. Geophys. Union, v. 87, n. 52, AGU Fall Meeting, Abstract U53A-0024.

Ranero, C. R., Phipps Morgan, J., McIntosh, K., and Reichert, C., 2003a. Bending, faulting, and mantle serpentinization at the Middle America trench, Nature, v. 425,p. 367-373.

Ranero, C. R., Weinrebe, W., Grevemeyer, L., Phipps Morgan, J., Vannucchi, P., and R. von Huene, 2003b. Tectonic structure of the Middle America Pacific Margin and Incoming Cocos plate from Costa Rica to Guatemala, EOS Trans. Amer. Geophys. Union, v. 84, n. 46, AGU Fall Meeting, Abstract T52C-0289.

Ranero, C.R., A. Villasenor, J. Phipps Morgan, and W. Weinrebe, 2005. Relationship between bend faulting at trenches and intermediate-depth seismicity. Geochem. Geophys. Geosyst, v.6, Q12002, doi:10.1029/2005GC000997.

Sandwell, D. T., and Smith, W. H. F., 1997. Marine gravity anomaly from Geosat and ERS 1 satellite altimetry. Journal of Geophysical Research, v. 102 , No. B5, p. 10039-10054.

Ségoufin, J.,Munschy. M., Bouysse, P., and Mendel, V., et al., 2004. Map of the Indian Ocean (1:20 000 000), sheet 1:"Physiography", sheet 2:"Structural map". CGMW Edition, Paris.

Sibuet, J.-C., Rangin, C., Le Pichon, X., Singh., S., Cattaneo, A., Graindorge, D., Klingelhoefer, F., Lin, J.-Y., Malod, J.A., Maury, T., Schneider, J.-L., Sultan, N., Umber, M., Yamagushi, H., and the "Sumatra aftershocks" team, (subm.). 26th December 2004 Great Sumatra-Andaman Earthquake : seismogenic zone and active splay faults, Earth and Planet. Sci. Lett.

Sibuet, J.C., Rangin, C., Le Pichon, X., Singh, S., Cattaneo, A., Graindorge, D., Klingelhoefer, F., Lin, J., Malod, J., Maury, T., Sultan, N., and Umber, M, 2006. 26th December 2004 Great Sumatra-Andaman Earthquake: seismogenic zone and active splay faults. EOS Trans. Amer. Geophys. Union, v. 87, n. 52, AGU Fall Meeting, Abstract U51B-03.

Sieh, K., and D.H. Natawidjaja, 2000. Neotectonics of the Sumatran Fault, Indonesia, J. Geophys. Res., v. 105 , No. B12, p. 28295-28326,.

Singh, S. and Sumatra-Aftershocks Team, 2005. Sumatra earthquake research indicates why rupture propagated northwards. EOS Trans. Amer. Geophys. Union, v. 86, n. 48, p. 497, 502.

Singh, S., Carton, H., Hartoyo, D., Hananto, N., Chauhan, A., Tapponnier, P., White, N., Bunting, T., Christie, P., Lubis, H., Martin, J., Klingelhoefer, F., 2006. Seismic reflection images of the Great Sumatra-Andaman earthquake rupture: from source to surface. EOS Trans. Amer. Geophys. Union, v. 87, n. 52, AGU Fall Meeting, Abstract U44A-04.

Suppe, J., 1983. Geometry and kinematics of fault-bend folding. Am. J. Sci., v. 283, p. 684-721.

Vigny, C., W.F.J. Simons, S. Abu, R. Bamphenyu, C. Satirapod, N. Choosakul, C. Subarya, A. Socquet, K. Omar, H.Z. Abidin, and B.A.C. Ambrosius, 2005. Insight into the 2004 Sumatra-Andaman earthquake from GPS measurements on southeast Asia, Nature, v. 436, p. 201-206.

von Huene, R., and C. R. Ranero, 2003. Subduction erosion and basal friction along the sediment-starved convergent margin off Antofagasta, Chile, J. Geophys. Res., v. 108, B2, 2079, doi:10.1029/2001JB001569.

Weinrebe, W., C. R. Ranero, J. Diaz, C. Reichert, and E. E. Vera, 2003. Continental margin tectonics along the convergent plate boundary of central Chile, Eos Trans. AGU, v. 84, n. 46, AGU Fall Meet., Abstract T31C-0859.

Wessel, P. and Smith, W. H. F. (1991). Free software helps map and display data. EOS Trans. AGU, 72:445-446.

**Figure Captions :**

Figure 1: Bathymetric image (shaded relief with illumination from the SW) of the NW Sumatra forearc, from the combined data set from 2005-2006 R/V Marion Dufresne surveys and the HMS Scott survey. Inset shows tectonic setting of the study area, with red star the epicenter of the 26 December 2004 earthquake.

Figure 2: Seafloor slope map of the study area. Flat slopes are white to blue, and steep slopes red (> 10°) and black (>20°).

Figure 3: Morphotectonic interpretation of the NW Sumatra forearc. Note landward vergence of thrusts at the toe of the accretionary wedge and ~N-S lineaments within both the upper and lower plates.

Figure 4: Close-up of N-S lineaments on incoming oceanic plate (Northern example) and corresponding 3.5 kHz seismic profiles across these lineaments (data from R/V Marion Dufresne cruise: Sumatra-OBS). Structures are interpreted as possibly reactivated bending-related normal faults.

Figure 5: (b) Close-up of N-S lineaments on incoming oceanic plate (Southern example) and corresponding 3.5 kHz seismic profiles across lineaments (data from R/V Marion Dufresne cruise: Sumatra-OBS). Structures are interpreted as bending related normal faults with a major left lateral strike slip motion. Inset (a) is an interpreted sketch of southern pull-apart basins indicating a hypothetical left lateral strike slip motion. This figure exhibits clearly the two sets of lineaments evidenced on the oceanic crust and their interaction.

Figure 6: (a) Free-air gravity map of study area (Sandwell and Smith, 1997), showing N-S trending fracture zones of the Indo-Australian plate. Focal mechanisms for strike slip events (red) and normal events (blue) are plotted from are from the CMT catalog (1976 to March 2007). The two black events are from Deplus et al, 1998. All the strike slip events for the forearc (in the accretionary wedge domain) and the oceanic domain are plotted. For normal and sub-normal events, only those from the oceanic domain are plotted.. (b) Close-up of the detailed bathymetry in the Wharton basin from the Samudra cruise (Deplus et al., 1998). Black dots indicate possible position of fossil spreading center from magnetic anomalies (Deplus et al., 1998).

Figure 7: 3D view (looking N15E along the Sunda trench) of toe region of accretionary wedge and hypothesised sub-surface structural geometry, with N-S lineaments on oceanic plate controlling segmentation of some of the thrust anticlines and positions of major erosional features. Note the major erosional features indenting the slopes ans superimposed on the fold. Note the asymmetry of the frontal folds.

**Figure 1**

**Click here to download high resolution image**

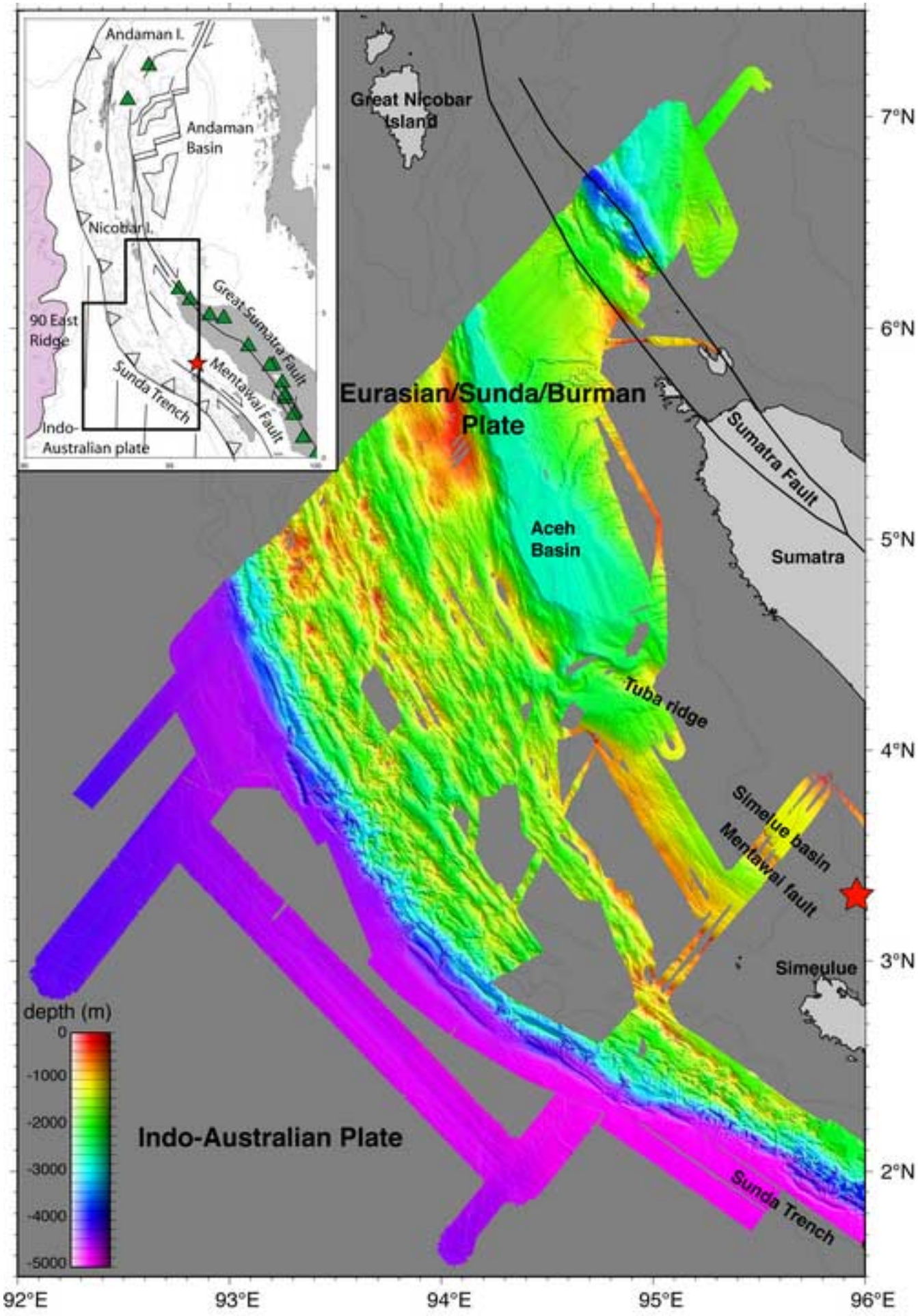

**Figure 2**

**Click here to download high resolution image**

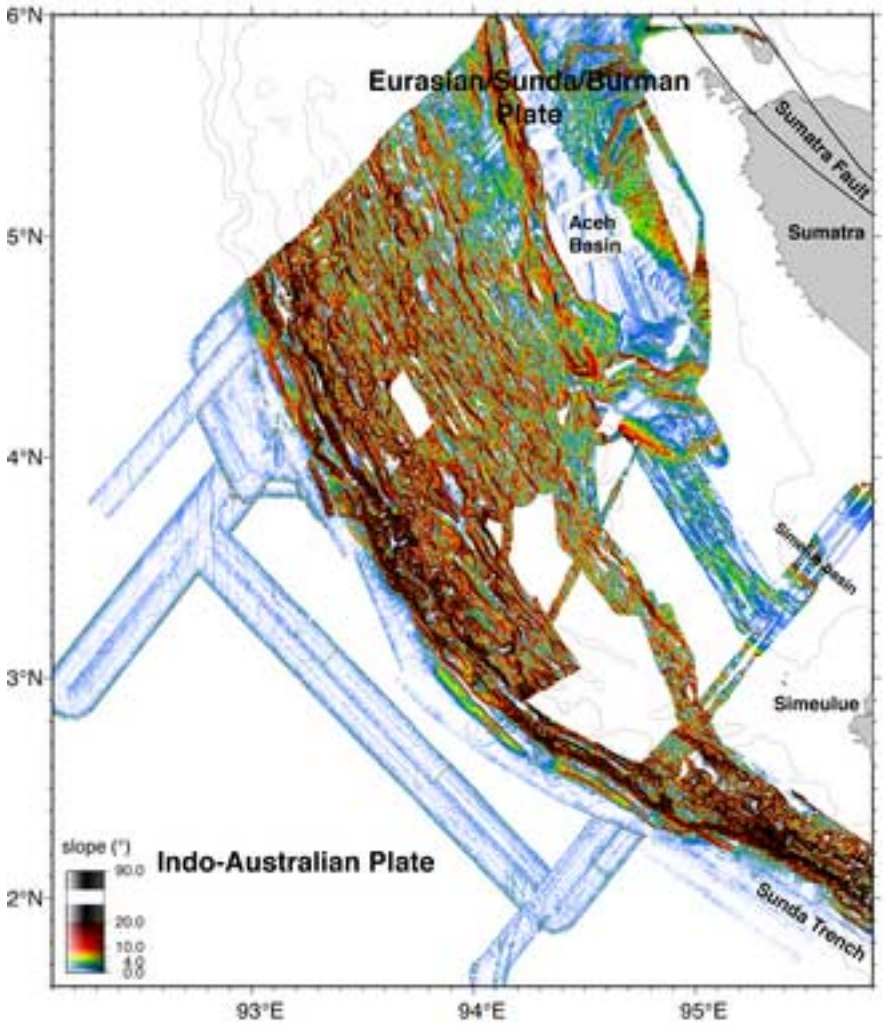

**Figure 3**

**Click here to download high resolution image**

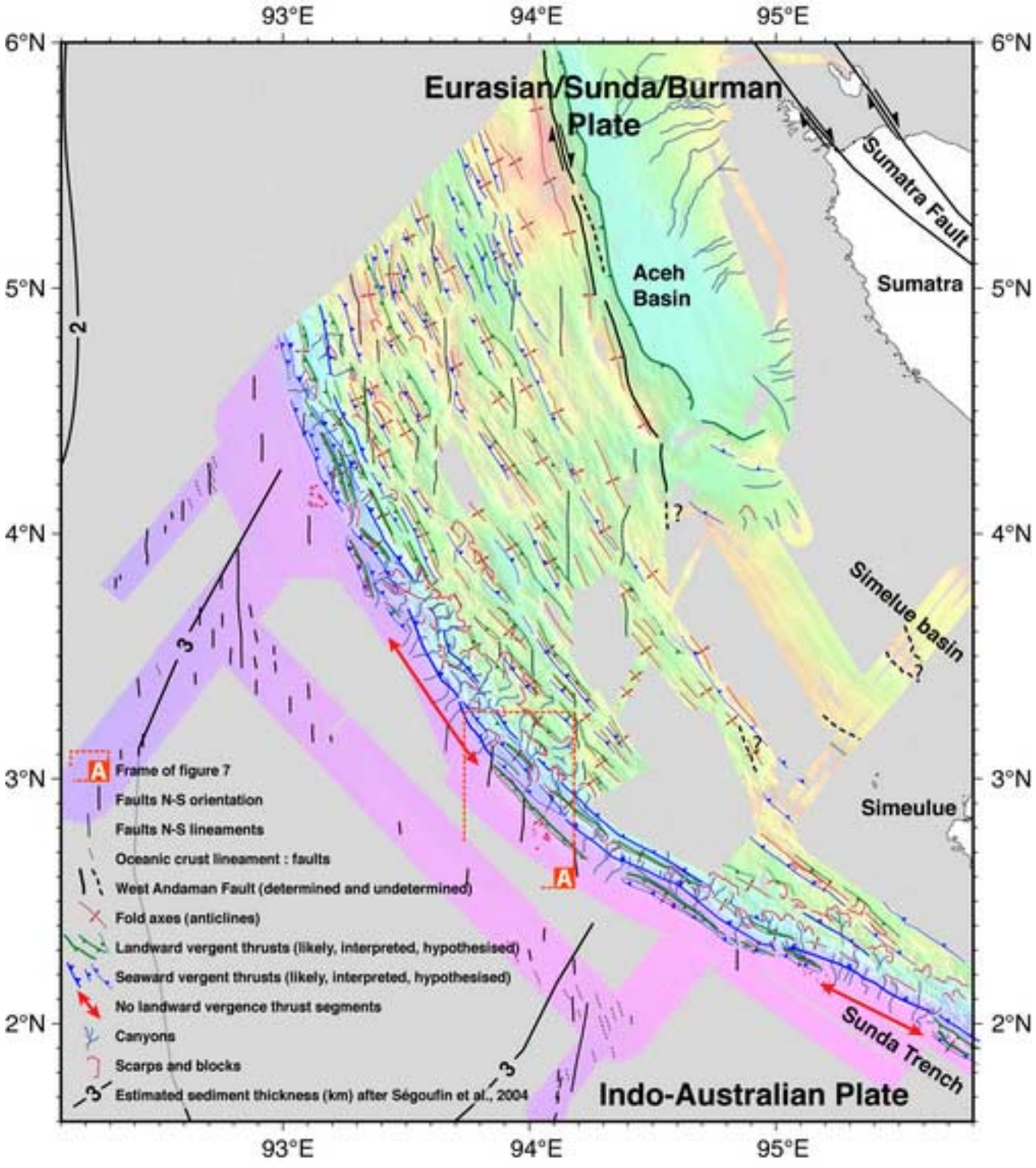

**Figure 4**

**Click here to download high resolution image**

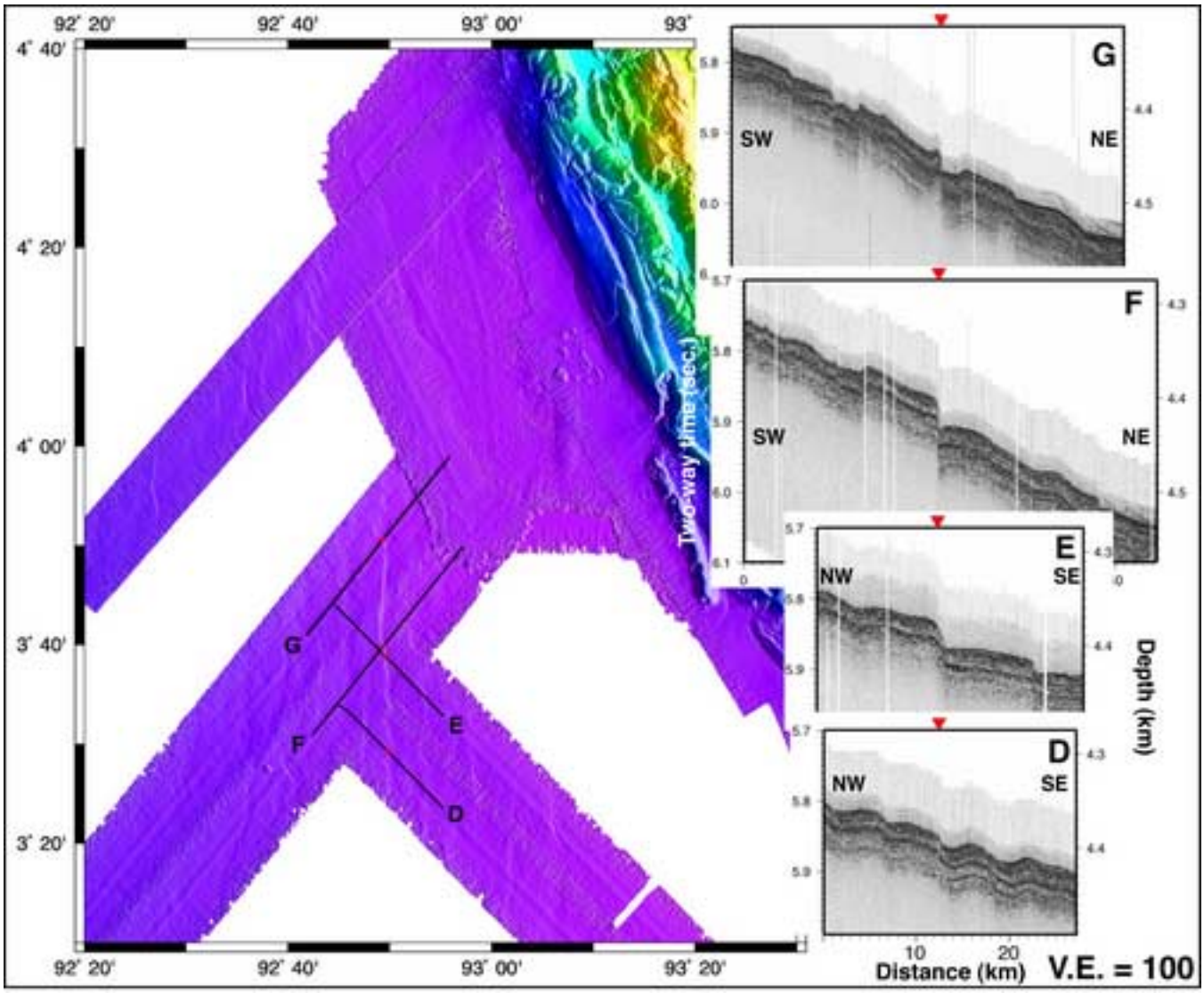

**Figure 5**

Click here to download high resolution image

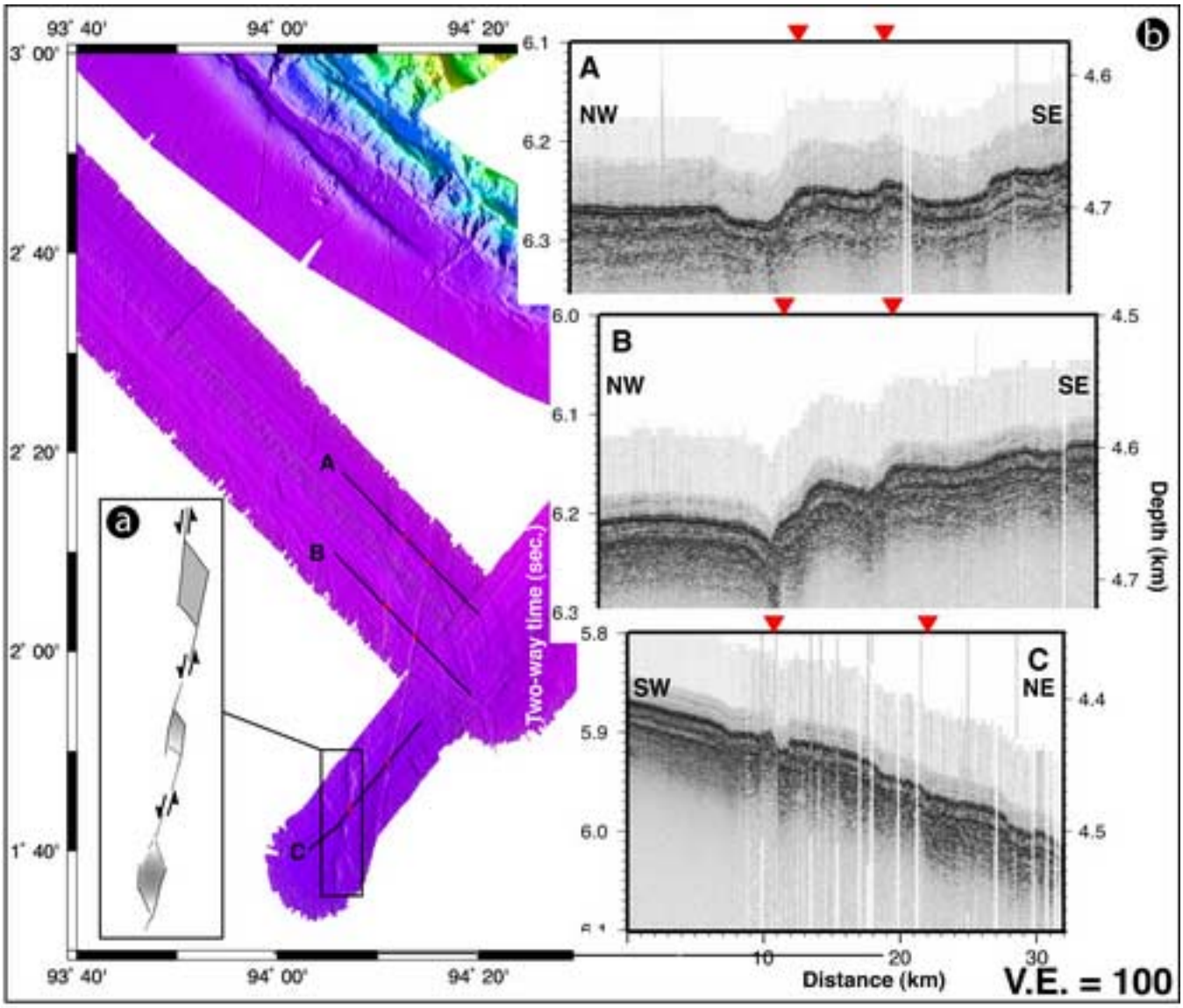

**Figure 6**

**Click here to download high resolution image**

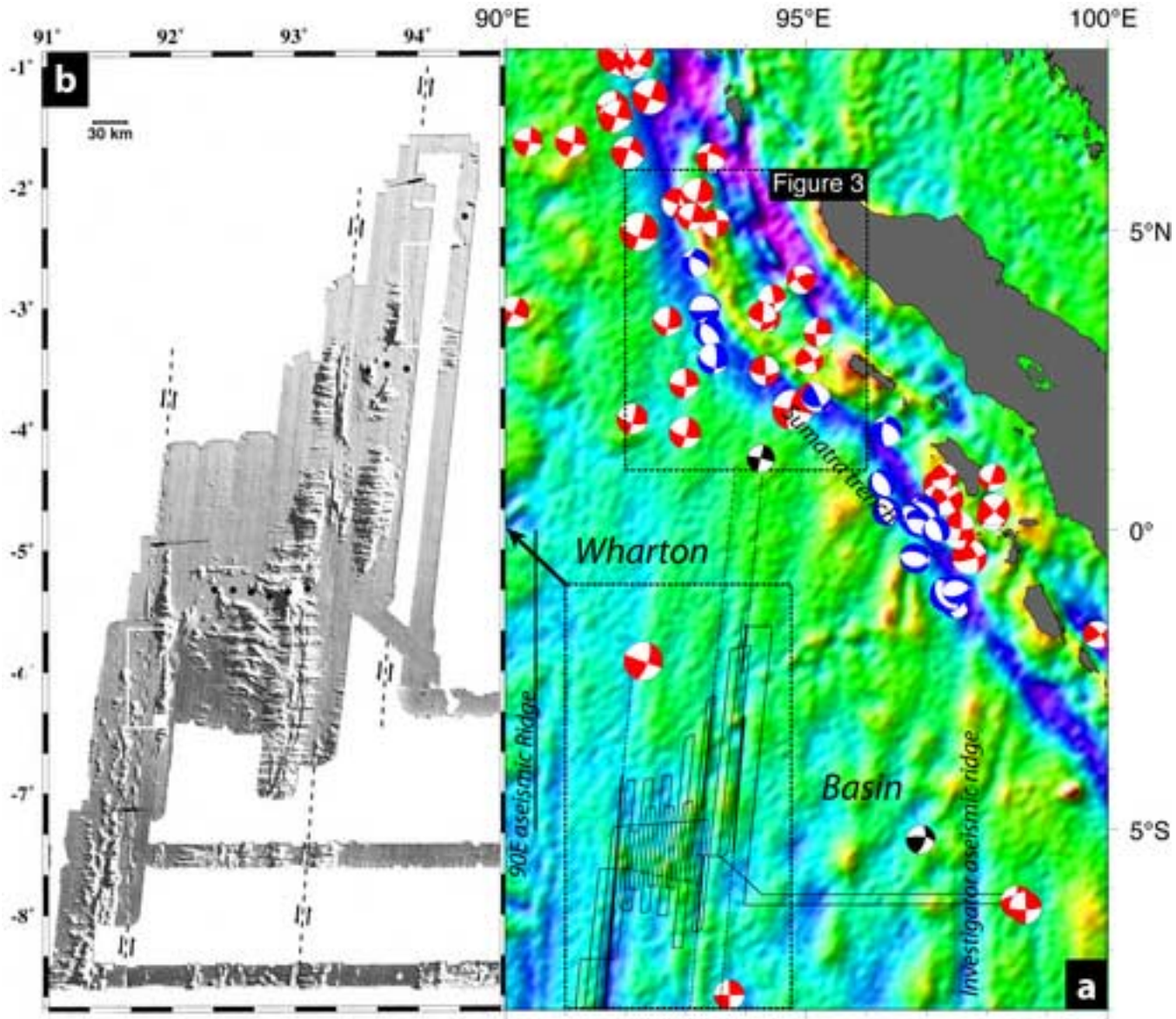

**Figure 7**

**Click here to download high resolution image**